Research Article Open Access

Aliye Arabacı*

Oxide ionic conductivity and microstructures of Pr and Sm co-doped CeO_2-based systems

https://doi.org/10.1515/chem-2018-0087
received January 22, 2018; accepted May 3, 2018.

Abstract: The compositions $Ce_{0.80}Sm_{0.2-x}Pr_xO_{2-\delta}$ (x=0-0.12) were prepared through the citrate-nitrate method. The synthesized Pr^{3+} and Sm^{3+} co-doped ceria powders with different compositions were calcined at 600°C for 3 h. Phase structure of the calcined powders was characterized by X-Ray diffraction (XRD) analysis. All the calcined samples were found to be ceria based solid solutions of fluorite type structures. The morphology examinations were carried out by scanning electron microscopy (SEM) analysis. Relative density of more than 91% of the theoretical can be achieved by sintering the $Ce_{0.80}Sm_{0.2-x}Pr_xO_{2-\delta}$ pellets at 1400°C for 6 h. The two-probe a.c. impedance spectroscopy was used to study the ionic conductivity of the doped ceria samples. The $Ce_{0.80}Sm_{0.08}Pr_{0.12}O_{1.90}$ composition showed the highest total ionic conductivity value which is 2.39×10^{-2} S/cm at 600°C.

Keywords: Solid Oxide Fuel Cells; X-Ray Diffraction; Co-Doped Ceria; Electrolyte.

1 Introduction

Energy is one of the important topics of humanity through ages and it became more important with developing technology. A large part of the world energy demand is met by fossil fuels. Fossil fuels are limited sources and they cause environmental pollution. For this reason, Researchers focus on alternative renewable energy sources such as wind energy and solar energy, etc. [1-4]. Among the alternative energy sources, Solid oxide fuel cells (SOFCs) attract attention.

SOFC are energy generation devices, which electrochemically convert chemical energy to electrical energy. SOFC have several advantages such as high efficiency, being environmentally friendly and great flexibility in fuel choice [5,6]. Electrolyte materials used for SOFCs are usually the main components determining the performance of the fuel cell. Conventional SOFCs based on yttria stabilized zirconia (YSZ) electrolyte usually operate at high temperatures (800-1000°C) to retain high oxygen ionic conductivity. However, high temperature operation causes difficulties in material selection and sealing, which blocks the commercial process of the SOFCs. One important need for commercialization of SOFCs is to lower their operating temperature, which requires an electrolyte that can operate at lower temperatures. Hence, the operating temperature of SOFC has to be reduced to eliminate the problems. Lowering the operating temperature from 800-1000°C to 400–700ºC would result in an increase in the cell stability and allow the usage of cost-effective materials for cell fabrication.

Ceria (CeO_2) doped with heterovalent cations, such as rare earth and alkaline earth ions is the most promising high-conducting solid electrolyte for intermediate temperature SOFC applications. In doped ceria, the lower valent (such as; Gd^{3+},Sm^{3+}) ions occupy the tetravalent cerium ion sites and create oxygen vacancies into the CeO_2 lattice to provide charge balance. This situation can be expressed using the Kröger-Vink notation [7,8]:

$$Sm_2O_3 \xrightarrow{2CeO_2} 2Sm'_{Ce} + 3\,O_o^x + V_o'' \quad (1)$$

$$O_o^x + 2\,Ce_{Ce^x} \rightarrow 2Ce_{Ce'} + {}^1/_2\,O_{2\,(gaz)} + V_o'' \quad (2)$$

Ceria doped with heterovalent cations, such as rare earth and alkaline earth ions have been extensively studied as the most promising electrolyte materials for intermediate temperature solid oxide fuel cells (IT-SOFC) [7,8]. Sm^{3+} is considered one of the best dopants for ceria-based solid electrolytes currently available [9]. On the other hand, ceria-based electrolytes easily develop n-type electronic conduction. At low oxygen partial pressures, Ce^{4+} in doped ceria tends to be reduced to Ce^{3+}. The reduction of ceria introduces free electrons responsible for mixed ionic-electronic conductivity. However, electronic conduction

***Corresponding author: Aliye Arabacı,** Istanbul University-Cerrahpasa, Faculty of Engineering, Department of Metallurgical and Materials Engineering, Avcilar, 34320 Istanbul, Turkey, E-mail: aliye@istanbul.edu.tr

in electrolyte material creates internal Ohmic loss. This situation will cause a decrease in the performance of SOFCs. In order to prepare appropriate doped ceria electrolyte materials for SOFC applications, the electrolytic domain of the electrolyte should be expanded to the oxygen partial pressure range suitable for SOFC operation. The electrolytic domain which is also termed as "the application region of the electrolyte", can be described as the oxygen partial pressure (PO_2) when semiconduction becomes the dominating conduction mechanism over the pure ionic conductivity [10].

Effort has been made to suppress the electronic conductivity and to extend the electrolytic domain of the ceria-based electrolytes. For example, Maricle et al. [11] reported that the addition of a small amount of Pr^{3+} in gadolinium-doped ceria $Ce_{1-x}Gd_xO_{2-x/2}$ (GDC) solid solutions decreases the electronic conductivity and leads to an extension of the electrolytic domain boundary. They also calculated the electronic conductivity from the total conductivity at low oxygen activities of $Ce_{0.8}Gd_{0.2-x}Pr_xO_{1.9}$ (x=0.001 to 0.06) in the temperature range 659–859°C with impedance spectroscopy and found for x=0.01 to 0.03 as the optimum Pr-level with respect to the decreased n-type conduction. Lubke and Wiemhöfer [12] studied Pr-doped GDC in detail and found that the p-type conductivity of the material could be increased by co-doping Pr. They also reported that the ionic conductivity may increase because of the decrease of grain boundary electrical resistance. Moreover, Lui et al. [13] documented that the SOFC with samaria and praseodymium co-doped ceria (SPDC) electrolyte had a higher power density but lower open circuit voltage. They noted that the performance of SOFCs with Sm-doped ceria electrolyte could be enhanced by co-doping with Pr in the electrolyte. They also reported that the improvement is created by the increased oxygen ionic conductivity of the electrolyte and the decreased polarization of the electrolyte–electrode interface. Briefly, Lui et al. summarized that the Pr dopant could modify the grain boundary behaviours so that the oxygen ionic conductivity of the electrolyte could be increased and the electrocatalytic activity of Pr could reduce the polarization resistance of the electrolyte-electrode interface.

According to the studies in literature, it can be clearly defined that the performance of SOFCs can be further improved if ceria co-doped with Pr and Sm (or Gd) is employed as an electrolyte material.

Among the ceria based electrolytes, samarium-doped ceria, $Ce_{0.8}Sm_{0.2}O_{1.9}$ was reported to have the highest ionic conductivity [7]. In our previous work [14], neodymium, erbium, and gadolinium co-doped Sm-doped ceria ($Ce_{0.8}Sm_{0.2}O_{1.9}$) samples were prepared by using the citric–nitrate combustion process method, providing low-temperature preparation and morphological control in ultrafine particles of uniform crystallite dimension. Citrate nitrate method which is a wet chemical process is able to produce ultrafine powders with narrow size distributions [15-17]. As well known, phase purity and relative density are important factors for obtaining high performance doped cerium oxide electrolytes. Therefore, in the present study, to produce high performance co-doped cerium oxide based electrolytes, combustion synthesis method was preferred.

This work concentrates on the compositions $Ce_{0.80}Sm_{0.20-x}Pr_xO_{2-\delta}$, denoted as SDC, PSDC6, PSDC9 and PSDC12 ($Ce_{0.80}Sm_{0.20}O_{1.90}$, $Ce_{0.80}Sm_{0.14}Pr_{0.06}O_{1.90}$, $Ce_{0.80}Sm_{0.11}Pr_{0.09}O_{1.90}$ and $Ce_{0.80}Sm_{0.08}Pr_{0.12}O_{1.90}$) which were prepared by using the citrate-nitrate combustion method. In this method, cerium, samarium and praseodymium nitrate salts were used as the starting materials and citric acid anhydrous was used as the fuel. Effects of co-doping on the structure and ionic conductivity were studied in comparison with the singly doped ceria ($Ce_{0.80}Sm_{0.20}O_{1.90}$, SDC). The total dopant cation amount was kept at 20 mol %.

2 Experimental

Samples with the general formula $Ce_{0.80}Sm_{0.2-x}Pr_xO_{2-\delta}$ were synthesized through the citrate-nitrate method. Cerium nitrate ($Ce(NO_3)_3$ x$6H_2O$, purity 99.99%, Sigma Aldrich), samarium nitrate ($Sm(NO_3)_3$ x$6H_2O$, purity 99.99%, Sigma Aldrich) and praseodymium nitrate ($Pr(NO_3)_3$ x$6H_2O$, purity 99.9%, Sigma Aldrich) were used as the starting materials. Citric acid anhydrous ($C_6H_8O_7$, Boehringer Ingelheim) was used as the fuel. 0.08 M of $Ce(NO_3)_3 \bullet 6H_2O$ and 0.02 M of $M(NO_3)_3 \bullet 6H_2O$ (M:Sm, Pr) were pre-dissolved in deionized water and then mixed into an aqueous solution at room temperature. The necessary amount of citric acid dissolved in de-ionized water was then added to the mixed metal nitrate solution with stirring. Mole ratio of total metal ions to citric acid was 1:1. During heating this mixture on a hot plate at 85°C for 2 h, the excess water and nitrate gases were removed to form a viscous gel. After heating for a longer time at 85°C, the gel swelled into avoluminous light brown foam and then auto-ignition of the light purple foam occurred, accompanied with the evolution of a large number of gaseous molecules. Afterwards, this foam was kept at 300°C for 1 h in a muffle furnace which led to decomposition of precursors. The residual powder was then calcined at 600°C for 3 h to obtain the final product. The samples calcined at 600°C were pressed using a cold isostatic press (CIP) at 200 MPa into pellets of 10 mm in diameter and 1.5 mm in thickness. Prepared

pellets were sintered at 1400°C for 6 h. Samples sintered at high temperature were used for density, FE-SEM and AC conductivity measurements.

XRD patterns of the samples were obtained with the Rigaku D/max-2200 PC branded XRD device using Cu-Kα (λ = 0.15406 nm) radiation at room temperature. XRD analyses were performed on the samples calcined in air at 600°C for 3 h. Morphological characteristics of the sintered pellets (1400°C for 6h) were investigated employing FEI-Quanta FEG 450 branded SEM.

The A.C. Impedance spectra of the samples were recorded using an AC impedance analyzer (Solartron 1260 FRA and 1296 Interface as a function of temperature (300-800°C) in air in the measuring frequency range from 100 MHz to 10 MHz. The impedance data was analyzed using the Zview software. In order to prepare the samples for the ionic conductivity measurements, both sides of the pellets were coated with silver paste to construct Ag| $Ce_{0.80}Sm_{0.20-x}Pr_xO_{1.90}$ |Ag cell and then heat treated at 800°C for 30 min. Conductivities of the samples were found by substituting the value of the resistances and dimensions of the samples in the Equation (3),

$$\sigma = L/SR_{Total} \quad (3)$$

where L is the sample thickness, R_{Total} ($R_{Total} = R_{gi}$ (the grain interior (lattice) resistance) + R_{gb} (the grain boundary resistance)) is the total resistance and S is the effective electrode area.

Temperature dependence of the conductivity can be expressed by the following Equation (4):

$$\sigma = \frac{\sigma_0}{T} exp^{-\frac{E}{kT}} \quad (4)$$

where T is the temperature (K), σ is the total conductivity at temperature T, σ_0 is a pre-exponential factor, E is the activation energy, and k is the Boltzmann's constant (k = 8.61 x 10^{-5} eV K^{-1}). σ_0 is related to the oxygen vacancy concentration and vibrational frequency of the lattice.

Ethical approval: The conducted research is not related to either human or animals use.

3 Results and Discussion

XRD patterns of the calcined $Ce_{0.80}Sm_{0.20-x}Pr_xO_{2-\delta}$ powders are shown in Figure1. All the calcined $Ce_{0.80}Sm_{0.20-x}Pr_xO_{2-\delta}$ powders exhibit only the cubic fluorite type crystal structure (JCPDS powder diffraction file no.34-0394). No secondary phases were observed in any of the specimens, indicating a complete solid solution for the $Ce_{0.80}Sm_{0.20-x}Pr_xO_{2-\delta}$ for all dopant concentration range. The addition of Sm_2O_3 and Pr_2O_3 into CeO_2 may cause a small shift in the X-ray peak reflections to lower 2θ values which is an evidence of an increase of the lattice parameter. The lattice parameter reached higher values with increasing dopant content due to the different radii of Ce^{4+} (0.096 Å), Pr^{3+}(1.126 Å) and Sm^{3+} (1.079 Å) in solid solutions of the fluorite-type structure. The doping effect leads to a change in the lattice plane spacing values and a shift of the diffraction peaks to new 2θ positions. The calculated lattice parameters of SDC, PSDC6, PSDC9 and PSDC12 were found as 5.428 Å, 5.435 Å, 5.437 Å and 5.439 Å, respectively. The crystallite size (D_{XRD}) was calculated according to the well-known Scherrer equation given in Equation (5);

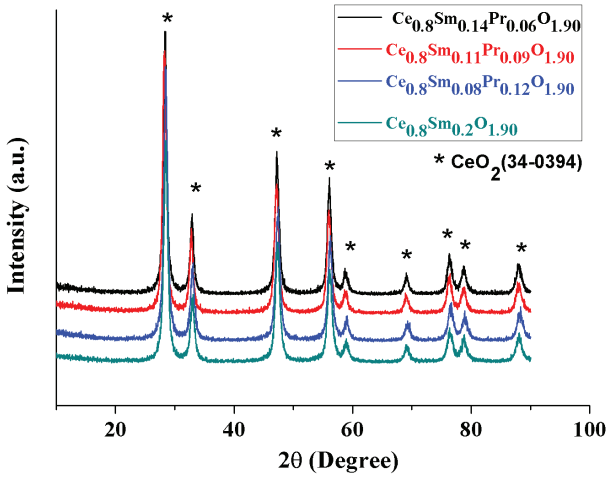

Figure 1: X-ray diffraction pattern of the powder samples $Ce_{0.80}Sm_{0.20-x}Pr_xO_{2-\delta}$ (x = 0, 0.06, 0.09, 0.12).

$$D_{XRD} = 0.9\lambda/\beta\cos\theta \quad (5)$$

where, λ is the wavelength of the radiation, θ presents the diffraction angle and β is the full width in radians at half maximum intensity of the powder pattern at 2θ. Crystallite sizes of the calcined powder samples calculated using the Scherrer Formula were determined as 12-14 nm.

Microstructure of the sintered $Ce_{0.80}Sm_{0.20-x}Pr_xO_{2-\delta}$ pellets was studied with the SEM. Typical micrographs of the surface of the sintered $Ce_{0.80}Sm_{0.20-x}Pr_xO_{2-\delta}$ pellets are shown in Figure 2. Sintered pellets had a dense structure and regular grain sizes. The SDC, PSDC6 and PSDC9 pellets had approximately similar grain sizes between 0.70, 0.75 and 0.72 μm, respectively. However, the PSDC12 pellet had a large grain size of 0.98 μm. This situation is consistent with the relative density values. The relative densities of the SDC, PSDC6, PSDC9 and PSDC12 samples were found as 92%, 91.4%, 91% and 94%, respectively.

The impedance spectrum of an ionic conductor contains contributions from the grain-interior, grain-boundary, and electrode–electrolyte interface, which can be simplified by three arcs. However, depending on the nature of the sample and experiment conditions not all of these arcs can be seen together [18]. These three arcs can be identified clearly below 500°C.

In fact, the total conductivity (σ_T) of rare-earth element doped ceria is the sum of ionic conductivity (σ_i) and electronic conductivity (σ_e). The main contribution of the conductivity of ceria-based compounds in air is the ionic conductivity and contribution of the electronic conductivity is negligible ($\sigma_i \approx 10^{-2}$ S/cm, $\sigma_e \approx 10^{-5}$ S/cm < 800°C) [7,8]. Whereas ceria doped with mixed-valence cation such as $Pr^{3+/4+}$ induce electronic conductivity yielding mixed conductivity properties which are ionic and p-type electronic conductivity [19,12].

Pure ceria is originally a poor oxide ion conductor. In doped ceria, the lower valent Sm^{3+} ions occupy the Ce^{4+} ion sites and introduce oxygen vacancies into the ceria lattice to provide charge balance. Ionic conduction in doped ceria takes place via an oxygen vacancy diffusion mechanism [20]. The ionic conductivities are significantly enhanced in doped ceria electrolytes by increasing the oxygen vacancies ($V_O^{\cdot\cdot}$) (see Eq.(1)). So, the ionic conductivity of $Ce_{1-x}Sm_xO_{1.9}$ system increases systematically with increasing samarium (due to formation of increasing oxygen vacancies) and reaches a maximum for the $Ce_{0.8}Sm_{0.2}O_{1.9}$ composition [7] and then decreases for high levels of samarium. The decrease in the ionic conductivity for a higher *x* value is attributed to the defect associations of the type $Sm'_{Ce}V_O^{\cdot\cdot}$ at higher concentrations of $V_O^{\cdot\cdot}$. The resistivity was converted into conductivity value according to Eq. (4).

In this study, in the $Ce_{0.80}Sm_{0.20-x}Pr_xO_{2-\delta}$ system, Pr substitutions do not provide additional oxygen vacancies, because Pr^{4+} or Pr^{3+} can substitute for Ce^{4+}/Sm^{3+}, as previously remarked by Greenblatt et al. [21]. In the $Ce_{0.80}Sm_{0.20-x}Pr_xO_{2-\delta}$ system, the possible redox process may be $Pr^{3+} \leftrightarrow Pr^{4+} + e^-$. By this redox process an electronic contribution to the total conductivity might be introduced in the system. Moreover, Greenblatt et al mentioned that at lower Pr amounts, owing to the redox potentials of Pr^{4+}/Pr^{3+} which are slightly higher than that of Ce^{4+}/Ce^{3+}, praseodymium would trap mobile electrons. Maricle et al. [11] reported similar results.

The complex impedance spectra of the $Ce_{0.80}Sm_{0.11}Pr_{0.09}O_{1.90}$ pellet measured at 300°C, 450°C and 700°C in an air atmosphere is shown in Figure3. The same trend was observed for all examined samples. In Figure 3a, three well-defined half-circular arcs, which denote the grain-interior (gi), grain-boundary (gb), and electrode (e) are visible. With increasing operating temperature (Figure 3b), the first half-circle (the high-frequency arc) disappears and only the grain-boundary and electrode arcs are discernible. When the temperature increases (Figure 3c), the grain-interior and grain-boundary resistances become frequency independent and solely one half-circle, which represents the electrode resistance, is visible. At 700°C, a single arc, which refers to the electrode, was observed.

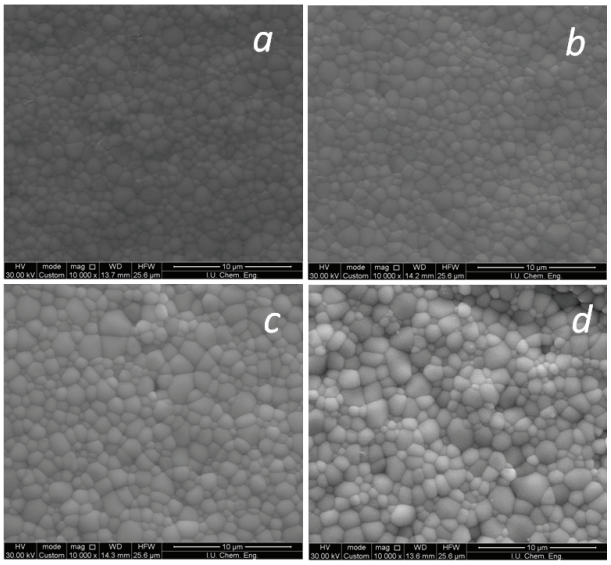

Figure 2: SEM micrographs of the SDC, PSDC6, PSDC9 and PSDC12 samples (X10.000).

Diffusion of the oxygen ions within the fluorite structure can be defined as a thermally activated process with characteristic activation energy (see Eq. (4)). The temperature dependence of the ionic conductivities of the $Ce_{0.80}Sm_{0.20-x}Pr_xO_{2-\delta}$ pellets sintered at 1400°C are given in Figure 4. As can be seen from Figure 4, above 600°C, the total conductivity increases with the increasing Pr amount owing to the increasing contribution of electronic conductivity to the total conductivity. Meaning that the total conductivity reaches the highest value with x=0.12 in the $Ce_{0.80}Sm_{0.2-x}Pr_xO_{2-\delta}$ system due to the increasing contribution of electrons to the transport process, as reported by Liu et al. [13]. Liu et al. explained that co-doping Pr in Sm-doped ceria may increase the oxygen ionic conductivity by changing the grain boundary conditions so that more oxygen vacancies may exist and move faster. They also stated that the electrochemical catalytic activity of Pr may play an important role on decreasing the polarization of electrolyte–electrode interface of the SOFCs.

As the grain size decreases, grain boundary path for ion conduction increases. However, in this study, the

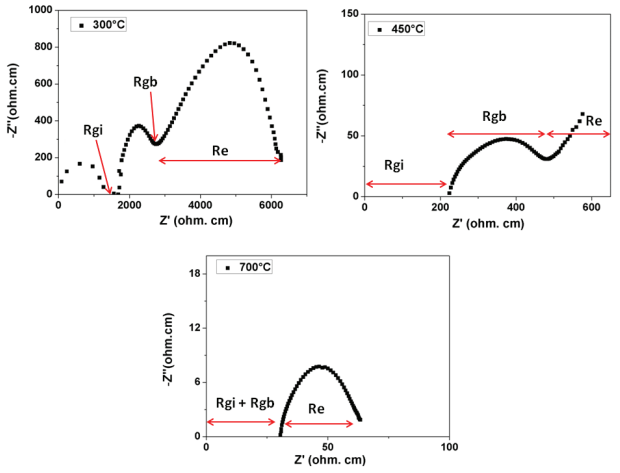

Figure 3: Complex impedance spectra plots of the PSDC9 pellet, measured at 300°C, 450°C and 700°C in air. The grain-interior, grain-boundary and electrode contributions are represented as Rgi, Rgb and Re, respectively.

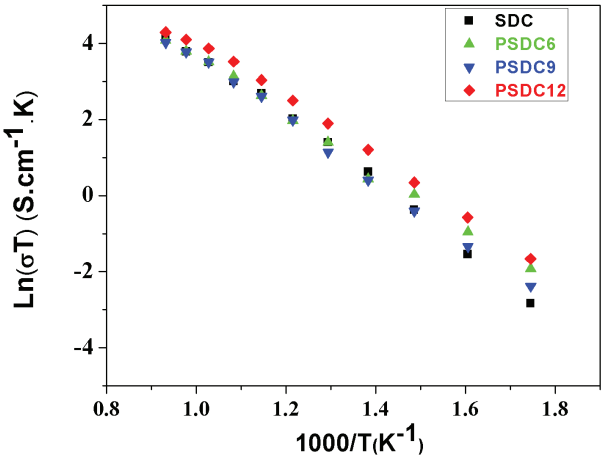

Figure 4: Arrhenius plots for the electrical conductivities of the $Ce_{0.80}Sm_{0.20-x}Pr_xO_{2-\delta}$ samples.

PSDC12 pellet had the biggest grain size which is 0.98 μm and therefore the smallest percentage of grain-boundary region results in the smallest grain-boundary resistivity. The difference in the grain-boundary resistivity of the $Ce_{0.80}Sm_{0.20-x}Pr_xO_{2-\delta}$ pellets influences the total conductivity.

In the present study, the PSDC12 pellet showed the highest conductivity at all measurement temperatures. For example, the total ionic conductivity of PSDC12 was 2.39×10^{-2} S/cm (0.64 eV) at 600°C and the total ionic conductivity of PSDC12 is 33% higher than SDC (1.79×10^{-2} S/cm (77 eV)). The PSDC12 pellet had a larger grain size (see in Figure2) and higher conductivity owing to the lower resistance of the grain-boundary of the pellet. These findings agree with the results of Kharton et al.

From the microstructural studies of the $Ce_{0.80}Gd_{0.18}Pr_{0.02}O_{2-d}$ ceramics that Kharton et al. [22] reported, it is seen that Pr doping increases the tendency for segregation of rare-earth dopants at the grain boundaries and the segregated Pr-enriched phase may have a positive effect on electrochemical activity.

4 Conclusion

Praseodymium and samarium co-doped ceria samples $Ce_{0.80}Sm_{0.20-x}Pr_xO_{2-\delta}$ (x=0, 0.06, 0.09 and 0.12) are synthesized through the citrate-nitrate method. It is clearly evident from the XRD pattern that all samples crystallize in cubic phase and therefore, only the peaks of CeO_2 phase were found. There are no secondary phases that belong to the dopants. Dense ceramics were obtained by sintering the pellets at 1400°C for 6 h. The relative densities of the samples are over 91% of the theoretical density and these results are consistent with the SEM studies. According to the electrochemical impedance spectroscopy results, the total ionic conductivity of PSDC12 (2.39×10^{-2} S/cm (0.64 eV)) is 33% higher than singly doped ceria, SDC (1.79×10^{-2} S/cm (77 eV)) at 600 °C. The low resistance of the grain-boundaries of the PSDC12 pellet improved the conductivity of the SDC pellet.

Acknowledgement: This research work was supported by the Research Fund of the Istanbul University, project No. 52750.

Conflict of interest: Authors state no conflict of interest.

References

[1] Yegeubayeva S.S., Bayeshov A.B., Bayeshova A.K., Electrochemical Method of Obtaining of Electric Current from Thermal Energy Using Graphite Electrodes, Acta Phys. Pol. A, 2015, 128, 455-457.

[2] Jadallah A.A., Mahmood D.Y., Er Z., Abdulqaedr Z.A., Hybridization of Solar/Wind Energy System for Power Generation in Rural Aeras, Acta Phys. Pol. A, 2016, 434-437.

[3] Evans A., Strezov V., Evans T.J. , Renew. Sust. Energ. Rev., 2009, 13(5), 1082-1088.

[4] Pişirira O. M. and Bingöl O., Industrial PC Based Heliostat Control for Solar Power Towers, Acta Phys. Pol. A, 2016, 130, 36-40.

[5] Nielsen J., Hagen A., Liu Y.L., Effect Of Cathode Gas Humidification On Performance And Durability Of Solid Oxide Fuel Cells, Solid State Ionics, 2010, 181, 517-524.

[6] Steele B. C. H., Material Science And Engineering: The Enabling Technology For The Commercialisation Of Fuel Cell Systems, J. Mater. Sci., 2001, 36(5), 1053-1068.
[7] Inaba H. and Tagawa H., Ceria-based solid electrolytes, Solid State Ionics, 1996, 83(1-2), 1-16.
[8] Steele B.C.H., Appraisal Of $Ce_{1-y}Gd_y O_{2-y/2}$ Electrolytes For IT-SOFC Operation At 500°C, Solid State Ionics, 2000, 129(1), 95-110.
[9] Eguchi K., Setoguchi T., Inoue T., Arai H., Electrical Properties Of Ceria-Based Oxides And Their Application to Solid Oxide Fuel Cells., Solid State Ionics,1992, 52(1-3), 165-172.
[10] Schneider D., Gödickemeier M., Gauckler L.J., Nonstoichiometry and Defect Chemistry Of Ceria Solid Solutions, J. Electroceram., 1997, 1(2), 165–172.
[11] Maricle D.L., Swarm T.E., Karavolis S., Enhanced Ceria- a Low-Temperature SOFC Electrolyte, Solid State Ionics,1992, 52(1-3), 173-182.
[12] Lübke S., Wiemhöfer H. D., Electronic Conductivity Of Gd-Doped Ceria With Additional Pr-Doping , Solid State Ionics, 1999, 117(3-4), 229–243.
[13] Ji Y., Liu J., He T., Wang J., Su W., The Effect of Pr co-dopant on the Performance of Solid Oxide Fuel Cells with Sm-doped Ceria Electrolyte, J. Alloy. Compd, 2005, 389(1-2), 317–322.
[14] Arabacı A., Effect Of Er, Gd, And Nd Co-Dopants On The Properties Of Sm-Doped Ceria Electrolyte For IT-SOFC, Metall. Mater. Trans. A, 2017, 48A(5), 2282- 2288.
[15] Purohit R. D., Sharma B.P., And Pillai K.T., Ultrafine Ceria Powders Via Glycine-Nitrate Combustion , Mater. Res. Bull., 2001, 36(15), 2711–2721.
[16] Mahata T., Das G., Mishra R.K., And Sharma B.P., Combustion Synthesis Of Gadolinia Doped Ceria Powder, J. Alloy. Compd., 2005, 391(1–2), 129–135.
[17] Lenka R. K., Mahata T., Sinha P.K., And Sharma B.P., Combustion Synthesis, Powder Characteristics, and Shrinkage Behavior of a Gadolinia–Ceria System, J. Am. Ceram. Soc., 2006, 89(12), 3871–3873.
[18] Zhang T. S., Ma J., Chen Y.Z., Luo L.H., Kong L.B., Chan S.H., Different Conduction Behaviors Of Grain Boundaries In SiO_2-Containing 8 YSZ and CGO20 Electrolytes , Solid State Ionics, 2006, 177(13-14), 1227–1235.
[19] Bishop S. R., Stefanik T.S., Tuller H.L., Electrical Conductivity and Defect Equilibria of $Pr_{0.1}Ce_{0.9}O_{2-\delta}$, Phys. Chem. Chem. Phys., 2011, 13(21), 10165– 10173.
[20] Kilner J.A., Fast Oxygen Transport In Acceptor Doped Oxides, Solid State Ionics, 2000, 129(1-4),13-23.
[21] Huang W., Shuk P., Greenblatt M., Hydrothermal Synthesis And Properties Of Terbium- Or Praseodymium-Doped $Ce_{1-x}Sm_xO_{2-x/2}$ Solid Solutions, Solid State Ionics, 1998, 113–115, 305-310.
[22] Kharton V. V., Viskup A.P., Figueiredo F.M., Naumovich E.N., Yaremchenko A.A., Marques F.M.B., Electrochemical properties of Pr-doped $Ce(Gd)O_{2-\delta}$, Mater. Lett., 2002, 53(3), 160–164.